

Search for new spin-1 boson using ATLAS detector data

X.G. Mapekula

University of Johannesburg, Johannesburg, Department of Mechanical Engineering, Corner Kingsway and University Road, Johannesburg, South Africa.

E-mail: xmapekul@cern.ch

Abstract. We present a search for a new spin-1 or spin-0 boson where the Standard Model Higgs boson decays into a four lepton final state ($l = \mu$ or e) corresponding to the $H \rightarrow Z_d Z_d \rightarrow 4\ell$. In this scenario, Z_d is the new boson found in the intermediate state, having a mass range of between 15 - 60 GeV. The search is conducted using pp collision data collected with the ATLAS detector at the LHC, where the total integrated luminosity corresponds to 139 fb^{-1} at a centre of mass energy of $\sqrt{s}=13 \text{ TeV}$. No significant deviation from the Standard Model was observed in the data. However, an improvement of a factor between two and four from the previous iteration of the analysis was observed for the limits that were set on the fiducial cross-section and the branching ratio of the Higgs boson. Limits were also set on the mixing parameter related to the Beyond Standard Model framework used in this analysis.

1 Introduction

The Higgs boson discovery at the LHC is the Standard Model (SM) missing component. However, observations of dark matter suggest otherwise because dark matter is not accounted for in the SM. Therefore, extensions to the Higgs sector of the SM favouring the existence of dark matter are highly motivated.

One way of extending SM is through exotic Higgs boson decays, where precision measurements have shown that Higgs boson properties allow for branching ratio $BR < 13\%$ for non-standard Higgs boson decays. It is also shown that since the Higgs Boson has a very narrow width, small couplings to a new light state should lead to a sizeable branching ratio. Furthermore, particles in the hidden sector are believed to prefer to couple to the Higgs boson, making it the preferred mediator between SM particles and the Hidden sector.

In the Hidden sector scenario [1–10], the addition of a $U(1)_d$ gauge symmetry [5–9] to the SM would mix kinetically with the $U(1)_Y$ hypercharge gauge with a coupling strength ϵ field. This mixing would make it possible to realize the mediation between the SM and the hidden sector. The dark photon Z_d would then be this symmetry's gauge boson. The mixing parameter ϵ determines Z_d boson's coupling strength to the SM, while gauge couplings determine Z_d boson decays. The branching ratio for Z_d decaying to muon and electron pairs can be 10%-15% [5] in the range $1 \text{ GeV} < m_{Z_d} < 60 \text{ GeV}$. The decays are prompt where $\epsilon \sim 10^{-5}$ [5] while for smaller values, Z_d decays would be significantly displaced. Furthermore, the decay width of the Z_d boson is very small for $\epsilon \leq 1$ and $m_{Z_d} < 60 \text{ GeV}$.

This paper presents the published Run 2 results [11] of the search for the Higgs boson decaying to four leptons via two Z_d bosons using pp data at $\sqrt{s} = 13 \text{ TeV}$ with an integrated luminosity

of 139 fb^{-1} collected using the ATLAS detector [12]. This analysis considers dark vector bosons decaying to same flavor muon and electron pairs, where $4e$, $2e2\mu$, and 4μ final states are included.

A brief description of the ATLAS detector, triggers, Monte Carlo simulation, pre-selection and event selection used in this analysis are given in Section 2. Contributions made by various background processes and the systematic uncertainties attached to them are described in Section 3. The results obtained from the analysis are described in Section 4 while Section 5 presents the paper’s conclusion.

2 Experimental Setup

The ATLAS detector, which covers a 4π solid angle with its cylindrical geometry, is a general-purpose detector situated on one of the four interaction points of the LHC.

Monte Carlo simulations are made with the ATLAS detector’s components in mind. In order to determine the expected shapes and yields of the signal and background events, we use Monte Carlo simulated samples. The simulations include pile-up and detector effects. The detector effects [13] are simulated using GEANT4 [14]. The signal samples related to the HAHM model [5,6,8,9] under consideration are simulated using MadGraph5 while the background events are simulated using Powheg box [15–19], Pythia [20], Madgraph5 [21] and Sherpa [22]. Small differences in data reconstruction, impact parameter efficiencies and isolation are corrected by applying weights to the simulated events.

2.1 Event Selection

We use event selection cuts to sift the signal events from the background events. We first require electrons to be located within the detector’s central region where $|\eta| < 2.47$ and $|z_0 \sin \theta| < 0.5 \text{ mm}$. The transverse momentum of each selected electron must be $p_T > 7 \text{ GeV}$. We require that muons be within the muon spectrometer’s acceptance region where $|\eta| < 2.7$. Similarly to the baseline electron requirements, $|z_0 \sin \theta| < 0.5 \text{ mm}$ and $p_T > 5$ (15) GeV for stand-alone (calo tagged) muons. We then look for quadruplets that have same flavor opposite sign pairs where the quadruplet with the smallest difference between the leading dilepton mass and the sub-leading dilepton mass is the one that is selected. The leptons in the quadruplet must be isolated from other deposits in the inner detector and the calorimeter. The invariant mass of the quadruplet must be within the Higgs window where $115 \text{ GeV} < m_H < 130 \text{ GeV}$. Finally, the quadruplet must comply with the medium signal region (MSR) requirement, which was previously defined by $m_{34}/m_{12} > 0.85$. This requirement was redefined in this iteration of the analysis because the background was sufficiently low at low energies ($\langle m_{\ell\ell} \rangle < 30 \text{ GeV}$) to search for a possible broader Z_d than was expected in the HAHM model. The MSR was then modified so that the Z_d width would be 3.5σ at the low end of the dilepton mass spectrum and decrease to 2.0σ at the higher end of the spectrum using Equation 1.

$$m_{34}/m_{12} > 0.85 - 0.1125f(m_{12}) \tag{1}$$

Where $f(m_{12})$ is the modulating function.

2.2 Signal

We generate the $H \rightarrow Z_d Z_d \rightarrow 4\ell$ process using the Hidden Abelian Higgs Model (HAHM) [9] with MADGRAPH5 [23] in conjunction with PYTHIA8 [24] which models hadronization, underlying event and parton shower. The dark vector boson Z_d mass is generated for values in the range 15 GeV and 60 GeV for various mass hypothesis values in steps 5 GeV for the process under consideration using the gluon-gluon fusion (ggF) production mode. The mass of the Higgs boson was set to 125 GeV. The cross-sections of the samples, which are next-to-next-to-leading-order, are normalized using $\sigma_{SM}(ggF) = 48.58 \text{ pb}$ as recommended in [25].

2.3 Backgrounds

- $H \rightarrow ZZ^* \rightarrow 4\ell$: We simulated Higgs production using POWHEG-BOX v2 MC event generator [18] for ggF [15], PDF4LHC NLO PDF set [26] for vector boson fusion [27] and vector boson [28]. MADGRAPH5_AMC@NLO [21] is used to simulate events produced via heavy quark annihilation while CT10nlo PDF set [29] and the NNPDF23 PDF set [30] are used to simulate events produced via $t\bar{t}H$ and $b\bar{b}H$ respectively. The ggF, VBF , VH and $b\bar{b}H$ production mechanisms were modeled using PYTHIA8 [31] for the $H \rightarrow ZZ^*$ decay process while the parton shower, multiple parton interactions and hadronization related to the decay process are modelled using the AZNLO parameter set. $t\bar{t}H$ showering is modeled using HERWIG++ [32] and the UEEE5 parameter set [33].
- $ZZ^* \rightarrow 4\ell$: The non-resonant SM $ZZ^* \rightarrow 4\ell$ process for quark anti-quark annihilation [34–36] was modeled using SHERPA 2.2.2 together with the NNPDF3.0 NNLO PDF set. The loop-induced gg process initiated ZZ^* production was modelled using GG2VV interfaced with PYTHIA8. The s-channel H diagrams were omitted using CT10 PDF’s in order to avoid double counting. The latter process was then calculated at LO. Because the latter process received large QCD corrections at NLO, it was multiplied by an NLO/LO K-factor of 1.70 ± 0.15 [37]. The $ZZ^* \rightarrow 4\ell$ background contributed 30% of the total background prediction.
- VVV/VBS: SHERPA 2.1 with the CT10 PDFs are used to model this process. The cross-sections of the processes, which include triboson production and vector boson scattering, are proportional to α^6 at leading order (LO). The results are four lepton final states, including two additional particles (electrons, quarks or muons). The Higgs production through VBF is subtracted from estimates obtained with this generator to avoid duplicates. This background contributed 17% of the total background.
- $Z + (t\bar{t}/J/\psi/\Upsilon) \rightarrow 4\ell$: We simulate the process where Z bosons are produced via a quarkonium state that decay to four leptons with PYTHIA8 with the NNPDF 2.3 PDF while POWHEG-BOX interfaced to PYTHIA6 [38] were used to simulate the $t\bar{t}H$ background.
- **Other Background**: Fake leptons produced from $Z + jets$, $t\bar{t}$ and WZ decay to less than four prompt leptons including jets. These are modeled using SHERPA 2.2 for $Z + jets$, POWHEG-BOX interfaced to PYTHIA6 [38] for $t\bar{t}$ production and POWHEG-BOX interfaced to PYTHIA8 and the CTEQ6L1 for WZ production.

3 Analysis procedure

3.1 Systematic uncertainties

Systematic uncertainties which were found to be dominant in this analysis include:

- **Luminosity and pileup**: We used the LUCID-2 detector [39] to obtain the uncertainties related to luminosity. This was found to be 1.7% [40] for the direct measurements of the luminosity. The measured and predicted inelastic cross section differences are used to determine the uncertainty due to pile-up, which accounts for about 1%.
- **Lepton-related uncertainties**: The event efficiency required to meet the selection criteria depends on lepton identification and reconstruction efficiencies and how well their momentum scale is determined. Momentum scales, resolutions for electrons and muons and efficiencies are measured by applying tag-and-probe techniques to the $Z \rightarrow \ell^+\ell^-$, $J/\psi \rightarrow \ell^+\ell^-$, and $\Upsilon \rightarrow \mu^+\mu^-$ dilepton resonances. Accounting for differences observed between simulation and data together with residual uncertainty estimations [41, 42] leads to corrections in the region of a percentage point. Small, single-lepton uncertainties in the final yield can lead to uncertainties in the region of 15% because the final state contains

four leptons. These uncertainties are usually dominated by electron identification and reconstruction efficiency.

- **Theoretical uncertainties:** In order to model uncertainties related to simulated signal and background processes, we vary the parton distribution functions, QCD scales, renormalization, factorization and modelling the underlying event and hadronization. This leads to a total uncertainty in signal acceptance of around 3 % while the background yield uncertainty is between 3–9% for $H \rightarrow ZZ^* \rightarrow 4\ell$ [43], and 5 % for $ZZ^* \rightarrow 4\ell$ [35–37, 44–46]

4 Results

This analysis has shown no significant excesses beyond SM. Therefore, we performed exclusion limits to interpret the results where model-independent limits are set on the fiducial cross-section. Model-dependent exclusion limits are set on the parameters of the benchmark model mentioned Section 1. The regions defined on generator-level quantities are used to derive the model-independent cross-section limits for this analysis. The fiducial event selection cuts are designed in such a way as to mimic the signal region selection cuts. The effects of the event selection are factorized into a primarily model-independent efficiency and a model-dependent acceptance using the fiducial event selections. The efficiency is thus used to determine the model-independent cross-section limit shown in Figure 2.

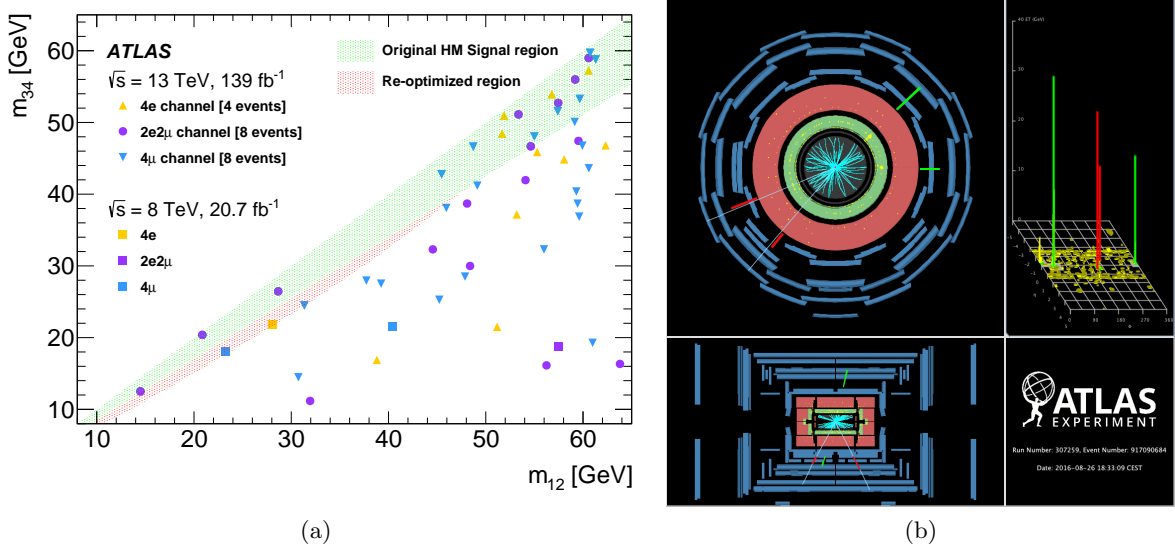


Figure 1: (a) Distribution of m_{12} vs m_{34} spectrum where the green region represents the previous MSR and the red region represents the new modulated MSR. The square marker represent the events from $\sqrt{s} = 8 \text{ TeV}$ data while the square and circle markers represent the $\sqrt{s} = 13 \text{ TeV}$ data. (b) Event display of one of the $2e2\mu$ events from the $\sqrt{s} = 13 \text{ TeV}$ data with $\langle m_{\ell\ell} \rangle = 27.5 \text{ GeV}$ that correspond to a global significance of 1.9σ

Although the analysis is statistically consistent with the SM, there is one event where $\langle m_{\ell\ell} \rangle < 15 \text{ GeV}$ and another two where $\langle m_{\ell\ell} \rangle > 60 \text{ GeV}$ which are possible candidates for Z_d . These are plotted in Figure 1a which shows the m_{12} vs m_{34} distribution. The largest deviations from the SM were found at $\langle m_{\ell\ell} \rangle = 28 \text{ GeV}$ and $\langle m_{\ell\ell} \rangle = 20 \text{ GeV}$ which have a local significance of 2.5σ and 1.9σ . The global significance of the event at $\langle m_{\ell\ell} \rangle = 28 \text{ GeV}$ was found to be 1.9σ . A similar analysis at the CMS collaboration also observed an event at 20 GeV with a

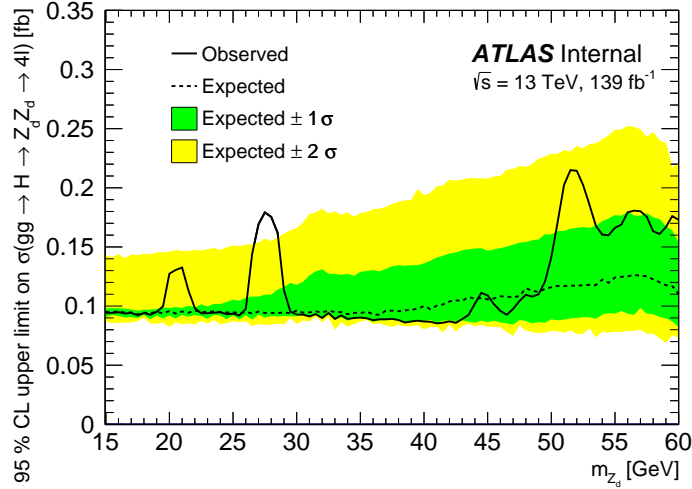


Figure 2: Observed and expected upper limits at 95% CL for the cross section of the $H \rightarrow Z_d Z_d \rightarrow 4\ell$ process, assuming SM Higgs boson production via the gluon-gluon fusion process. All final states are combined.

higher significance, shown in Figure 5b of in [47]. This is an interesting result which motivates a further probe for Run3. The profile likelihood ratio $\left(-2\log \frac{L(\mu=0, \hat{\theta})}{L(\hat{\mu}, \hat{\theta})}\right)$ was used as the test statistic to determine the significance values. The m_{12} vs m_{34} distribution shown is a new plot which includes the results for a previous search at 8 TeV [48]. This search also had Z_d candidates at a similar level of significance. In this paper, we have focused on the possible Z_d candidates, and so the event display of a typical one is also shown in Figure 1b.

5 Conclusion

This paper presents the search for the exotic decay of the 125GeV SM Higgs Boson to two dark vector bosons, which decay into a four-lepton final state. Data from the ATLAS experiment from the LHC, corresponding to 139 fb^{-1} of pp collision data at $\sqrt{s} = 7 \text{ TeV}$ was used in this analysis. This search was conducted in the mass range $15 \text{ GeV} < m_{Z_d} < 60 \text{ GeV}$. The data was found to be consistent with the predicted backgrounds. No significant deviations from SM were observed. Therefore limits were set on various parameters in the model.

References

- [1] Fayet P 2004 *Phys. Rev. D* **70** 023514 (*Preprint hep-ph/0403226*)
- [2] Finkbeiner D P and Weiner N 2007 *Phys. Rev. D* **76** 083519 (*Preprint astro-ph/0702587*)
- [3] Arkani-Hamed N, Finkbeiner D P, Slatyer T R and Weiner N 2009 *Phys. Rev. D* **79** 015014 (*Preprint 0810.0713*)
- [4] Dudas E, Mambrini Y, Pokorski S and Romagnoni A 2012 *JHEP* **10** 123 (*Preprint 1205.1520*)
- [5] Curtin D, Essig R, Gori S and Shelton J 2015 *JHEP* **02** 157 (*Preprint 1412.0018*)
- [6] Curtin D, Essig R, Gori S, Jaiswal P, Katz A *et al.* 2014 *Phys. Rev. D* **90** 075004 (*Preprint 1312.4992*)
- [7] Davoudiasl H, Lee H S, Lewis I and Marciano W J 2013 *Phys. Rev. D* **88** 015022 (*Preprint 1304.4935*)
- [8] Wells J D 2008 "" (*Preprint 0803.1243*)
- [9] Gopalakrishna S, Jung S and Wells J D 2008 *Phys. Rev. D* **78** 055002 (*Preprint 0801.3456*)
- [10] Alexander J *et al.* 2016 Dark Sectors 2016 Workshop: Community Report (*Preprint 1608.08632*)
- [11] ATLAS Collaboration 2021 (*Preprint 2110.13673*)
- [12] Collaboration" A 2005 *Phys. Rev. Lett.* **95** ISSN 00319007 URL <https://cds.cern.ch/record/391176/files/cer-0317330.pdf>
- [13] ATLAS Collaboration 2010 *Eur. Phys. J. C* **70** 823 (*Preprint 1005.4568*)
- [14] GEANT4 Collaboration, Agostinelli S *et al.* 2003 *Nucl. Instrum. Meth. A* **506** 250
- [15] Hamilton K, Nason P, Re E and Zanderighi G 2013 *JHEP* **10** 222 (*Preprint 1309.0017*)
- [16] Hamilton K, Nason P and Zanderighi G 2015 *JHEP* **05** 140 (*Preprint 1501.04637*)
- [17] Alioli S, Nason P, Oleari C and Re E 2010 *JHEP* **06** 043 (*Preprint 1002.2581*)
- [18] Nason P 2004 *JHEP* **11** 040 (*Preprint hep-ph/0409146*)
- [19] Frixione S, Nason P and Oleari C 2007 *JHEP* **11** 070 (*Preprint 0709.2092*)
- [20] Sjöstrand T, Ask S, Christiansen J R, Corke R, Desai N, Ilten P, Mrenna S, Prestel S, Rasmussen C O and Skands P Z 2015 *Comput. Phys. Commun.* **191** 159 (*Preprint 1410.3012*)
- [21] Alwall J, Frederix R, Frixione S, Hirschi V, Maltoni F, Mattelaer O, Shao H S, Stelzer T, Torrielli P and Zaro M 2014 *JHEP* **07** 079 (*Preprint 1405.0301*)
- [22] Bothmann E *et al.* 2019 *SciPost Phys.* **7** 034 (*Preprint 1905.09127*)
- [23] Alwall J, Herquet M, Maltoni F, Mattelaer O and Stelzer T 2011 *JHEP* **06** 128 (*Preprint 1106.0522*)
- [24] Sjöstrand T, Mrenna S and Skands P Z 2008 *Comput. Phys. Commun.* **178** 852–867 (*Preprint 0710.3820*)
- [25] Andersen J R *et al.* (LHC Higgs Cross Section Working Group) 2013 Handbook of LHC Higgs Cross Sections: 3. Higgs Properties (*Preprint 1307.1347*)
- [26] Butterworth J *et al.* 2016 *J. Phys. G* **43** 023001 (*Preprint 1510.03865*)
- [27] Nason P and Oleari C 2010 *JHEP* **02** 037 (*Preprint 0911.5299*)
- [28] Luisoni G, Nason P, Oleari C and Tramontano F 2013 *JHEP* **10** 083 (*Preprint 1306.2542*)
- [29] Lai H L *et al.* 2010 *Phys. Rev. D* **82** 074024 (*Preprint 1007.2241*)
- [30] Ball R D *et al.* 2013 *Nucl. Phys. B* **867** 244 (*Preprint 1207.1303*)
- [31] Sjöstrand T, Mrenna S and Skands P 2008 *Comput. Phys. Commun.* **178** 852–867 (*Preprint 0710.3820*)
- [32] Bähr M *et al.* 2008 *Eur. Phys. J. C* **58** 639 (*Preprint 0803.0883*)
- [33] Seymour M H and Siodmok A 2013 *JHEP* **10** 113 (*Preprint 1307.5015*)
- [34] Gleisberg T *et al.* 2009 *JHEP* **02** 007 (*Preprint 0811.4622*)
- [35] Gleisberg T and Höche S 2008 *JHEP* **12** 039 (*Preprint 0808.3674*)
- [36] Cascioli F, Maierhöfer P and Pozzorini S 2012 *Phys. Rev. Lett.* **108** 111601 (*Preprint 1111.5206*)
- [37] Caola F, Melnikov K, Röntsch R and Tancredi L 2015 *Phys. Rev. D* **92** 094028 (*Preprint 1509.06734*)
- [38] Sjöstrand T, Mrenna S and Skands P Z 2006 *JHEP* **05** 026 (*Preprint hep-ph/0603175*)
- [39] Avoni G *et al.* 2018 *JINST* **13** P07017
- [40] ATLAS Collaboration 2019 Luminosity determination in pp collisions at $\sqrt{s} = 13$ TeV using the ATLAS detector at the LHC ATLAS-CONF-2019-021 URL <https://cds.cern.ch/record/2677054>
- [41] ATLAS Collaboration 2019 *JINST* **14** P12006 (*Preprint 1908.00005*)
- [42] ATLAS Collaboration 2021 *Eur. Phys. J. C* **81** 578 (*Preprint 2012.00578*)
- [43] Dittmaier S *et al.* (LHC Higgs Cross Section Working Group) 2011 *CERN-2011-002* (*Preprint 1101.0593*)
- [44] ATLAS Collaboration 2017 Multi-Boson Simulation for 13 TeV ATLAS Analyses ATL-PHYS-PUB-2017-005 URL <https://cds.cern.ch/record/2261933>
- [45] Schumann S and Krauss F 2008 *JHEP* **03** 038 (*Preprint 0709.1027*)
- [46] Höche S, Krauss F, Schönherr M and Siegert F 2013 *JHEP* **04** 027 (*Preprint 1207.5030*)
- [47] CMS Collaboration 2020 Search for a low-mass dilepton resonance in Higgs boson decays to four-lepton final states at $\sqrt{s} = 13$ TeV CMS-PAS-HIG-19-007 URL <https://cds.cern.ch/record/2718976>
- [48] ATLAS Collaboration 2015 *Phys. Rev. D* **92** 092001 (*Preprint 1505.07645*)